https://doi.org/10.5194/acp-2022-751
Preprint. Discussion started: 4 January 2023

Atmospheric Chemistry and Physics Discussions

Measurement Report: Rapid decline of aerosol absorption coefficient and aerosol optical properties effects on radiative forcing in urban areas of Beijing from 2018 to 2021

Xinyao Hu[1,2], Junying Sun[1,3*], Can Xia[1,4], Xiaojing Shen[1], Yangmei Zhang[1], Quan Liu[1], Zhaodong Liu[1,4], Sinan Zhang[1], Jialing Wang[1], Aoyuan Yu[1,2], Jiayuan Lu[1], Shuo Liu[1], and Xiaoye Zhang[1]

[1]State Key Laboratory of Severe Weather & Key Laboratory of Atmospheric Chemistry of CMA, Chinese Academy of Meteorological Sciences, Beijing 100081, China

[2]University of Chinese Academy of Sciences, Beijing 100049, China

[3]State Key Laboratory of Cryospheric Science, Northwest Institute of Eco-Environment and Resources, Chinese Academy of Sciences, Lanzhou 730000, China

[4]Nanjing University of Information Science & Technology, Nanjing 210044, China

**Correspondence to*: Junying Sun (jysun@cma.gov.cn)

Abstract

Reliable observations of aerosol optical properties are crucial for quantifying the radiative forcing of climate. The simultaneous measurements of aerosol optical properties at three wavelengths for PM_1 and PM_{10} were conducted in urban Beijing from March 2018 to February 2022. The results showed considerable reductions in aerosol absorption coefficient (σ_{ab}) at 550 nm of PM_{10} and PM_1 by 55.0% and 53.5% from 2018 to 2021. SSA increased from 0.89 ± 0.04 for PM_{10} (0.87 ± 0.05 for PM_1) in 2018 to 0.93 ± 0.03 for PM_{10} (0.91 ± 0.04 for PM_1) in 2021. These results indicated that the absorbing aerosols were more effectively controlled than scattering aerosols due to pollution control measure-taking.

https://doi.org/10.5194/acp-2022-751
Preprint. Discussion started: 4 January 2023


Atmospheric Chemistry and Physics Discussions

The annual average submicron absorption ratio (Rab) increased from 86.1% in 2018 to 89.2% in 2021, suggesting that fine particles are the main contributors to total PM_{10} absorption and that the fine particles to absorption became more important. Absorption Angstrom exponent (AAE) in winter decreased from 2018 to 2021, implying a decreasing contribution from brown carbon to light absorption, which may relate to the decreased emissions of biomass burning and coal combustion. During the study period, aerosol radiative forcing efficiency became more negative and were −27.0 and -26.2 W m^{-2} AOD^{-1} for PM_{10} and PM_1 in 2021, which was mainly influenced by increasing SSA. Higher σ_{ab} and $PM_{2.5}$ mass concentrations were mainly distributed in clusters 4 and 5 transported from the south and the west of Beijing in each year. σ_{ab} and $PM_{2.5}$ corresponding to clusters 4 and 5 decreased evidently from 2018 to 2021, which may result from the control of source emissions in surrounding regions of Beijing. The 4-year data presented in this study provide critical optical parameters for radiative forcing assessment within two size ranges and are helpful for evaluating the effectiveness of clean air action.

1 Introduction

Atmospheric aerosols perturb the Earth's atmospheric radiation balance and climate forcing by directly affecting the scattering and absorption of solar radiation (Charlson et al., 1992; Jacobson, 2001) but also indirectly affecting cloud reflectivity and precipitation processes (Twomey, 2007). Light-scattering aerosols contribute to offsetting the warming effect of CO_2, while absorbing aerosols contribute to the heating of the atmosphere (Bond and Bergstrom, 2007), and produce a positive radiative forcing (Segura et al., 2016). The largest contribution to aerosol absorption is from black carbon (BC), which absorbs strongly over the entire solar spectrum (Bond and Bergstrom, 2007). Dust and brown

https://doi.org/10.5194/acp-2022-751
Preprint. Discussion started: 4 January 2023


Atmospheric Chemistry and Physics Discussions

carbon (BrC) are also light absorption aerosols, which strongly absorb in the ultraviolet (UV) spectrum. Globally, aerosols contributed an effective radiative forcing (ERF) of –1.3 ± 0.7 W m^{-2}, and the ERF due to emissions of BC is now estimated to be 0.11 (–0.20 to 0.42) W/m^2 between 1750 to 2019 (Szopa et al., 2021). However, aerosol properties are highly spatial and temporal variation, which results in radiative forcing variation from local to global scales and creates an observational challenge (Collaud Coen et al., 2013; Ealo et al., 2018; Andrews et al., 2011). Therefore, reliable observations of aerosol optical properties are crucial for quantifying the radiative forcing of climate.

In order to assess the role of aerosols on climate forcing accurately, a set of parameters that describe aerosol's optical properties are needed, such as scattering coefficient (σ_{sp}), absorption coefficient(σ_{ab}), and single scattering albedo (SSA). SSA is a key variable that determines the magnitude and the sign of the aerosol forcing (J. Hansen et al., 1997; Lee et al., 2007; Li et al., 2022a; Zhang et al., 2020). Previous study found that typical values of SSA are between 0.8 and 1 at worldwide locations (Dubovik et al., 2002), with higher values indicating a tendency towards a cooling effect (Li et al., 2022a). Besides, aerosol optical properties are wavelength-dependent, absorption Angstrom exponent (AAE) describes the spectral dependence of light absorption by aerosols and is typically used to differentiate between different aerosol types (Helin et al., 2021). The AAE for fresh BC is ~1, indicating "weak" spectral dependence of light absorption (Bond et al., 2013; Bond and Bergstrom, 2007), and the AAE >1 indicates the presence of BrC or dust, which tend to exhibit absorption that increases sharply as wavelength decreases (Moosmüller et al., 2009; Lack and Cappa, 2010). Thus, obtaining the aerosol absorption coefficient at different wavelengths is essential and can be helpful to differentiate between different aerosol types.

https://doi.org/10.5194/acp-2022-751
Preprint. Discussion started: 4 January 2023


Atmospheric Chemistry and Physics Discussions

As one of the world's most populous and rapidly developing megacities, Beijing experienced rapid economic growth and urbanization, accompanied by severe air pollution. Many in-situ measurements of aerosol optical properties have been conducted in Beijing (Bergin et al., 2001; He et al., 2009; Garland et al., 2009; Jing et al., 2015; Wang et al., 2019; Zhao et al., 2019; Xia et al., 2020). Previous studies found that high aerosol loading leads to large σ_{ab} in Beijing (Jing et al., 2015; Garland et al., 2009; Bergin et al., 2001). Moreover, the AAE showed significant seasonal variations in Beijing. Significantly higher AAE in winter than in summer highlights the important role of absorption of non-BC components (e.g. BrC) in winter (Xie et al., 2020; Xia et al., 2020). In order to reduce emissions and improve air quality, the government implemented strict pollution control measures (Xu and Zhang, 2020). Significant decreases in $PM_{2.5}$ mass concentrations were found in Beijing and the annual mean elemental carbon (EC) concentrations declined from 4.0 to 2.6 μg m^{-3} from March 2013 to February 2018 in Beijing (Ji et al., 2019). Xia et al. (2020) separated and quantified the effects of emission control and meteorological transport variability on BC loading from 2015 to 2017 in north China Plain. However, the environmental effects caused by emission controls are related to not only their mass concentrations, but also their optical properties and radiative effect (Luo et al., 2020). Therefore, it's necessary to investigate the multiple-year variations in aerosol optical properties and radiative effect in providing a comprehensive understanding of the effects of emission control. Wang et al. (2019) found that σ_{ap} for $PM_{2.5}$ decreased from 2014 to 2017, with a significant decrease of σ_{ap} in autumn. Sun et al. (2022) estimated that the direct radiative forcing of BC decreased by 67% from +3.36Wm^{-2} in 2012 to +1.09 Wm^{-2} in 2020. However, these studies were mostly conducted with conventional total suspended

https://doi.org/10.5194/acp-2022-751
Preprint. Discussion started: 4 January 2023


Atmospheric Chemistry and Physics Discussions

particulate (TSP) cyclone, $PM_{2.5}$ size cut, or PM_{10} size cut. Few studies focused on the sub-micron and super-micron particle optical properties and estimated aerosol radiative effect in the post-"Action Plan on Prevention and Control of Air Pollution" era. Acquiring the aerosol optical for the total (< 10μm diameter) and submicron aerosol is also in line with the aerosol advisory group of the Global Atmosphere Watch recommendation (WMO/GAW, 2016).

In this study, the simultaneous measurements of aerosol optical properties at three wavelengths for PM_1 and PM_{10} were conducted in urban Beijing from March 2018 to February 2022. The annual, seasonal, and diurnal variations of aerosol optical properties for two size cuts were investigated. The scattering properties of aerosols for two size ranges (PM_{10} and PM_1) under dry conditions observed in Beijing have been analyzed in detail by Hu et al. (2021). Thus, this study mainly focused on the variation of aerosol absorption coefficient, single scattering albedo, and absorption Angstrom Exponent for PM_{10} and PM_1. Moreover, the aerosol radiative effects in two size cuts were estimated. Finally, the transport and its impact on aerosol optical properties were analyzed. The 4-year data presented in this study provide key optical parameters for radiative forcing assessment within two size ranges and are helpful for evaluating the effectiveness of clean air action.

2 Instrumentation and methods

2.1 Site description

The sampling site in this study is located on the roof of the Chinese Academy of Meteorological Sciences (CAMS, 116°19′ E, 39°57′ N) in Beijing, which is a typical urban site in the northwest of Beijing between the 2nd and 3rd ring roads. The laboratory is

https://doi.org/10.5194/acp-2022-751
Preprint. Discussion started: 4 January 2023


Atmospheric Chemistry and Physics Discussions

approximately 53 m above ground level. The site is mainly influenced by local emission from residential living and traffic pollution (Xia et al., 2019).

2.2 Aerosol absorption measurements

The ambient air was sampled into a PM_{10} impactor with 16.7 LPM and then to an adsorption aerosol dryer, which controlled the relative humidity (RH) of sample air below 30% (Tuch et al., 2009). The dried aerosol sample passes through switched impactors that toggle the aerosol size cut between 1.0 µm (<1 µm) and 10 µm (<10 µm) aerodynamic particle diameters every 30 min, thus allowing to measure both fine and coarse particles (Hu et al., 2021). The sample aerosol was then passed into the Nephelometer (TSI Inc., Model 3563) and Tricolor Absorption Photometer (TAP, Brechtel Manufacturing, Inc., Hayward, CA, USA).

TAP measures absorption coefficient (σ_{ab}) at 465, 520, and 640 nm with the 47 mm diameter, glass-fiber filter and is a commercially available version of the continuous light absorption photometer (CLAP), which is low cost and high sensitivity (Ogren et al., 2017). The TAP comprises eight sample spots and two reference spots. The aerosol-laden air passes through one sample spot at a time, which allows for 8 times the filter lifetime compared to single-spot photometers (Davies et al., 2019). Unlike the Multi-Angle Absorption Photometer (MAAP), TAP does require a co-located aerosol light scattering or extinction measurement to derive aerosol light absorption (Ogren et al., 2017). Thus, simultaneous observation of aerosol light scattering has been measured and used to correct absorption data. When the Nephelometer and TAP were calibrated or malfunctioning, no data are available. During this study, 84% of the data was effective.

https://doi.org/10.5194/acp-2022-751
Preprint. Discussion started: 4 January 2023


Atmospheric Chemistry and Physics Discussions

2.3. Data processing

The TAP measures the light transmitted through a filter as particles are deposited onto the filter. The filter attenuation coefficient (σ_{atn}), at a specific wavelength (λ), can be determined as:

$$\sigma_{atn}(\lambda)=\frac{A}{Q}\times\frac{\Delta atn(\lambda)}{\Delta t} \quad (1)$$

where $\Delta atn\ (\lambda)$ is the filter attenuation at times t1 and t2, A is the area of on the filter, and Q is the sample flow rate through the filter.

In order to correct the error caused by multiple scattering and filter loading, the aerosol light absorption coefficient ($\sigma_{ab}\ (\lambda)$) was corrected based on the methods of Bond et al. (1999) and Ogren et al. (2017). First, the effect of filter loading was calibrated based on Eq. (2):

$$\sigma_{ab}(\lambda)\_raw=\frac{0.85\times\sigma_{atn}(\lambda)}{K_2\times(1.0796\times Tr(\lambda)+0.71)} \quad (2)$$

Then, $\sigma_{ab}\ (\lambda)$_raw at 465, 520, and 640 nm were adjusted to the wavelength of the light scattering coefficient based on the calculated AAE. Finally, the multiple scattering effect was corrected based on Eq. (3):

$$\sigma_{ab}(\lambda)=\sigma_{ab}(\lambda)\_raw-\frac{K_1\times\sigma_{sp}(\lambda)}{K_2} \quad (3)$$

where Tr (λ) is the normalized filter transmittance at time t relative to transmittance at the start of sampling (t =0) and σ_{sp} is the aerosol light-scattering coefficient at 450, 550, and 700 nm measured by the nephlometer. K_1 and K_2 were derived by Bond et al. (1999) as K_1 =0.02±0.02 and K_2 =1.22±0.20, where the uncertainties are given for the 95% confidence level.

https://doi.org/10.5194/acp-2022-751
Preprint. Discussion started: 4 January 2023


Atmospheric Chemistry and Physics Discussions

Using the corrected absorption coefficient data, the following parameters were calculated:

Absorption Angstrom exponent (AAE) describes the spectral dependence of light absorption.

$$AAE = -\frac{\ln(\sigma_{ab}^{\lambda 1}/\sigma_{ab}^{\lambda 2})}{\ln(\lambda 1/\lambda 2)} \quad (4)$$

The submicron absorption ratio (Rab) is determined as the ratio of the absorption coefficients for PM_1 and PM_{10}.

$$Rab = \frac{\sigma_{ab}(D<1\mu m)}{\sigma_{ab}(D<10\mu m)} \quad (5)$$

where σ_{ab} (D<1 μm) and σ_{ab} (D<10 μm) are σ_{ab} for particle diameters <1 μm and 10 μm, respectively.

Aerosol radiative forcing efficiency (RFE) at top-of-the-atmosphere (TOA) is a simplified formula that describes how large of an impact the aerosols would make to the aerosol radiative forcing (ΔF) per unit of aerosol optical depth (AOD) (Sheridan and Ogren, 1999) and we estimated the RFE at TOA as the Eq.6 (Haywood and Shine, 1995; Sheridan and Ogren, 1999):

$$RFE = \frac{\Delta F}{AOD} = -DS_0T_{at}^2(1-A_C)\times SSA\times\beta\times((1-R_s)^2-(\frac{2R_S}{\beta})\times(\frac{1}{SSA}-1)) \quad (6)$$

where D is the fractional day length, S_0 is the solar constant, T_{at} is the atmospheric transmission, Ac is the fractional cloud amount, and Rs is the surface reflectance. The constants used were D = 0.5, So = 1370 Wm^{-2}, T_{at} = 0.76, Ac = 0.6, and Rs = 0.15 as suggested by Haywood and Shine (1995), and upper scatter fraction β was calculated from $\beta = 0.0817+1.8495\times b-2.9682\times b^2$. backscatter ratio (b) was calculated based on scattering

https://doi.org/10.5194/acp-2022-751
Preprint. Discussion started: 4 January 2023


Atmospheric Chemistry and Physics Discussions

coefficient (σ_{sp}) and backscattering coefficient (σ_{bsp}) measured by Nephelometer as b = σ_{bsp}/ σ_{sp}. Equation (6) has been widely used to assess the intrinsic radiative forcing efficiency of aerosols at the top of the atmosphere (Sheridan and Ogren, 1999; Virkkula et al., 2011; Shen et al., 2018). In this study, the values of ΔF at TOA were also caculated by multiplying the RFE for PM_{10} with the AOD of ambient atmospheric aerosols observed at the CAMS site during the study periods. AOD can be downloaded from Aerosol Robotic Network (AERONET). Note that RFE was at a dry state, thus the ΔF at TOA here may be slightly underestimated.

2.4. Other data used

The hourly $PM_{2.5}$ and PM_{10} mass concentrations were measured at Guan yuan station, which is about 3km from the CAMS site. The data can be derived from the national air quality real-time publishing platform (http://106.37.208.233:20035/).

2.5. Back trajectories analysis

To investigate the influence of air mass origins on aerosol optical properties, 48-h backward trajectories arriving at Beijing at a height of 500 m above ground level were calculated from 0:00 to 23:00 local time each day from March 2018 to February 2022, using the Trajstat Software, combined with HYSPLIT 4 model (Hybrid Single-Particle Lagrangian Integrated Trajectory), and the NCEP Global Data Assimilation System (GDAS) data with a 1° × 1° resolution (Draxler and Hess, 1998; Wang et al., 2009).

In this study, four seasons are defined as follows: spring from March to May, summer from June to August, autumn from September to November, and winter from December to the following February, and all data are reported in Beijing time (UTC+8).

https://doi.org/10.5194/acp-2022-751
Preprint. Discussion started: 4 January 2023


Atmospheric Chemistry and Physics Discussions

3 Results and discussion

3.1 Temporal variation of aerosol optical properties

Figure 1 shows the annual variation of σ_{ab}, SSA, Rab, and $PM_{2.5}$ mass concentration from 2018 to 2021. During the study period, the annual mean $PM_{2.5}$ in 2018 was 54.7 μg m^{-3}, and it decreased by 34.4% (35.9 μg m^{-3}) in 2021, which suggested that the strict pollution control measures are effective in reducing the PM loadings in Beijing (Lei et al., 2021). σ_{ab} at 550 nm of PM_{10} and PM_1 showed similar annual variations. The annual mean σ_{ab} at 550 nm of PM_{10} and PM_1 decreased by 55.0% and 53.5%, respectively. A significant decrease in σ_{ab} indicated the effective control of absorbing aerosols, which was mainly related to decreasing biomass burning and coal consumption, increasing usage of natural gases, and the implementation of a stricter vehicular emission standard in recent years (Sun et al., 2022). The annual mean σ_{ab} for PM_{10} and PM_1 in 2021 was 9.8 Mm^{-1} and 8.7 Mm^{-1}, which were both lower than the result observed in Nainital, in the GH region, India (Dumka et al., 2015), but both higher than SMEAR II station located in Hyytiälä, southern Finland (Luoma et al., 2019). SSA is a key variable in assessing the aerosol radiative forcing. The variation of SSA also reflects the the ratio of aerosol scattering to total extinction with aerosol composition changes. The annual variations of SSA for PM_{10} and PM_1 were similar. During 2018-2021, annual mean SSA at 550 nm increased from 0.89 ± 0.04 for PM_{10} (0.87 ± 0.05 for PM_1) in 2018 to 0.93 ± 0.03 for PM_{10} (0.91 ± 0.04 for PM_1) in 2021, which demonstrated that the absorbing aerosols were effectively controlled compared to scattering aerosols during the past four years. On the other hand, increasing SSA also implied that scattering aerosols play a more important role in radiative forcing in urban Beijing. The mean submicron absorption ratio (Rab) increased yearly during the same

https://doi.org/10.5194/acp-2022-751
Preprint. Discussion started: 4 January 2023


Atmospheric Chemistry and Physics Discussions

period. It was from 86.1% in 2018 to 89.2% in 2021, suggesting that fine particles are the main contributors to total PM_{10} absorption, and the contributions from fine particles to absorption became more important.

The σ_{ab}, SSA, and AAE for PM_1 and PM_{10} showed similar annual variations in all seasons (Fig. 2 and Fig. S1). Thus, if not stated otherwise, the following discussion takes the aerosol optical properties of PM_{10} as an example. As shown in Fig. 2 seasonal average of σ_{ab} presented a decreasing trend during all seasons from 2018 to 2021, reflecting the reduction of absorbing aerosols which were related to effective control of absorbing aerosols emissions in Beijing. σ_{ab} decreased by half in autumn and winter during the study period, which was probably due to reducing coal consumption as a heating source and the reduction of biomass burning. In particular, σ_{ab} for PM_1 and PM_{10} decreased even up to 63% and 67% in the summer from 2018 to 2021. Traffic is a relatively stable source of absorption aerosols in summer (Li et al., 2022b). The largest deduction of σ_{ab} was in summer and could be related to more strict vehicle emission standards (Zhang et al., 2019).

In general, AAE was lowest in summer and highest in winter. The mean values of AAE for PM_{10} were 1.13 and 1.41 in summer and winter, respectively, similar to result at an urban site in Beijing in 2018 (Xie et al., 2020). During summer, the average AAE was generally close to 1, which suggested that BC from traffic emissions was the major component of light-absorbing aerosols. Li et al. (2022b) found that the percentage of liquid fuel (traffic) contributing to the total BC was 86.8% in summer in Beijing. The highest AAE suggested that BrC contributed to light absorption strongest in winter, which is due to enhanced emissions from biomass burning and coal combustion in winter (Sun et al., 2018). Notably, AAE decreased in winter from 1.48 for PM_{10} (1.48 for PM_1) in 2018 to

https://doi.org/10.5194/acp-2022-751
Preprint. Discussion started: 4 January 2023


Atmospheric Chemistry and Physics Discussions

1.37 for PM_{10} (1.34 for PM_1) in 2021 (Fig. 2 and Fig. S1), indicating a decreasing contribution from BrC to light absorption, which may relate to the effect control of biomass burning and coal combustion caused by changes in heating energy structure (Ji et al., 2022). To improve air quality, the Beijing-Tianjin-Hebei region adjusted the energy structure during the heating period and developed clean heating projects, such as the "coal to gas" project (Zhao et al., 2020; Liu et al., 2019). During the whole period, AAE was similar in spring and autumn indicating that light-absorbing aerosols were from similar emission sources in spring and autumn (Ran et al., 2016). AAE slightly increased in spring and autumn from 2018 to 2021. Part of the reason was the occurrence of multiple fugitive dust in spring and autumn (Yi et al., 2021; Gui et al., 2022). On the other hand, BrC could also be formed from secondary reactions (Bond et al., 2013; Wang et al., 2022). A slight increase in AAE in spring and autumn may also have been caused by a greater amount of secondary organic aerosol formation as a result of an increased atmospheric oxidation capacity (Ji et al., 2019; Lei et al., 2021).

The seasonal mean SSA showed an increasing trend in all seasons from 2018 to 2021, indicating that the contribution of scattering aerosols to extinction increased. This suggested that more effective control of scattering aerosols should be attached more importance in order to improve visibility in the future. In particular, SSA in winter increased significantly from 0.88 in 2018 to 0.93 in 2021, which revealed that the proportion of absorbing aerosols decreases considerably in winter. This is consistent with recent research which suggests that air pollution control measures has been more effective in reducing the primary pollution emissions than secondary species (Vu et al., 2019; Sun et al., 2020). On the other hand, seasonal mean SSA for PM_{10} was 0.94±0.04, 0.94±0.04,

https://doi.org/10.5194/acp-2022-751
Preprint. Discussion started: 4 January 2023


Atmospheric Chemistry and Physics Discussions

0.92± 0.04, 0.93±0.03 in spring, summer, autumn, and winter 2021. Similar SSA suggests that the proportions of light absorbing and scattering components became relatively stable in four seasons.

Figure 3 shows the diurnal variations of σ_{ab} and SSA at 550 nm for PM_{10}, which are similar to those for PM_1 (Figure. S2). In the past four years, σ_{ab} was lower during the day and higher at night in four seasons. This was consistent with that observed at an urban site in Beijing during 2014-2016 (Wang et al., 2019). The evolution of the planetary boundary layer had an important influence on the diurnal variation of the σ_{ab}. With stronger solar radiation, the boundary layer was more fully developed during the daytime, and after sunset, the convective boundary layer underwent a transition to the nocturnal stable boundary layer (Guo et al., 2016). Furthermore, emissions also affected the diurnal variation of the σ_{ab}. For example, heavy-duty diesel trucks and heavy-duty vehicles were only allowed to enter urban areas from 23:00 to the following day 06:00 (Hu et al., 2021). As a response, the minimum σ_{ab} occurred during 12:00–18:00, when the planetary boundary layer was well-developed, and truck emission was lower. With shallow boundary layer height and enhanced emissions from heavy-duty trucks, σ_{ab} reached the maximum at night. During the study period, SSA showed a significant peak in the afternoon in four seasons, which was similar to previous studies in urban Beijing (Zhao et al., 2019; Wang et al., 2019). Higher SSA was shown in the afternoon, which was mainly related to the reduction of absorbing aerosols emission, and more secondary scattering aerosol produced by strong chemical reactions under intensive solar radiation and high temperature in the afternoon (Han et al., 2017).

https://doi.org/10.5194/acp-2022-751
Preprint. Discussion started: 4 January 2023


Atmospheric Chemistry and Physics Discussions

3.2 Aerosol radiative effect

To study the climate impact of the aerosol particles, we investigated the variation of aerosol radiative forcing efficiency (RFE) at the top-of-the-atmosphere (TOA) variations. As seen in Fig. 4, RFE for PM_{10} and PM_1 were always negative during the whole observation period, suggesting that the aerosols measured in urban Beijing have a stable cooling effect on the climate. RFE for PM_{10} and PM_1 were −27.0 and -26.2 W m^{-2} AOD^{-1} in 2021 in urban Beijing, which was slightly negative than that of −24.9 W m^{-2} AOD^{-1} in Nanjing (Shen et al., 2018) and highly negative than that of −19.9 W m^{-2} AOD^{-1} in Finland (Virkkula et al., 2011). This suggested that the aerosols in urban Beijing have a higher cooling efficiency. RFE was affected by SSA and backscattering ratio (b) and we investigated the RFE variations with SSA and b in Beijing. As shown in Fig. 5, When SSA increases from 0.7 to 0.92, the mean RFE increases by 1.59 times, suggesting that SSA plays an important role in strengthening cooling efficiency. When SSA>0.92, the mean RFE relatively keeps constant. The approximate constant RFE does not mean that the absolute aerosol radiative forcing is constant; it just suggests that the intrinsic nature of the aerosol will not significantly affect the calculation of RFE (Andrews et al., 2011). Also, the backscattering ratio has a negative relationship with RFE. A lower values of backscattering ratio corresponds to larger particles (Luoma et al., 2019). RFE became more negative with increasing b, suggesting that smaller particles would cool the atmosphere more efficiently. During the study period, SSA increased from 0.89 to 0.93, while the yearly mean value of b was 0.13 every year during the study period. RFE became more negative from 2018 to 2021, suggesting that the efficiency of the aerosol cooling atmosphere was higher, which was mainly influenced by increasing SSA.

https://doi.org/10.5194/acp-2022-751
Preprint. Discussion started: 4 January 2023


Atmospheric Chemistry and Physics Discussions

The ratio of ΔF/AOD is known as the aerosol radiative forcing efficiency (RFE) and ΔF at TOA was caculated by multiplying the RFE for PM_{10} with the AOD of ambient atmospheric aerosols observed at the CAMS site during the study periods. The mean value of ΔF from 2018-2021 was -15.0 W m^{-2}, -12.5 W m^{-2}, -12.1 W m^{-2}, and -11.8 W m^{-2}, respectively. Although RFE became more negative, the annual mean ΔF in 2021 corresponding to lower columnar aerosol loading became less negative than that of 2018 corresponding to higher columnar aerosol loading (Fig. S3) which was consistent with the analysis that aerosol loading was a essential factor for the estimation of ΔF (Andrews et al., 2011; Delene and Ogren, 2002).

3.3 Transport and its impact on aerosol optical properties in Beijing

In order to explore the influence of regional transports and the potential source regions of pollutants, we analyzed the air mass back-trajectories. The air mass back trajectories during 2018–2021 were calculated and clustered (Fig. 7); then, we statistic the aerosol optical properties of each cluster from 2018-2021 (Fig. 8). Based on the Euclidean distance, the back trajectories were classified into five clusters, in which clusters 1, 2 and 3, which originated from the clean areas in Mongolia and eastern Inner Mongolia, and transported to Beijing along the pathway with low emissions, were corresponded to low σ_{ab} and low $PM_{2.5}$ (Fig. 8a, d). Cluster 4 from the south of Beijing and cluster 5 from the west of Beijing were referred to as the polluted air masses, and the average $PM_{2.5}$ concentrations and σ_{ab} of clusters 4 and 5 were higher than those of clusters 1, 2, and 3 in each year (Fig. 8a, d). Cluster 4 passed through Shandong and Hebei Province, which was heavily polluted before arriving in Beijing. Cluster 5 passed through polluted Shanxi and Hebei during transport. SSA of cluster 4 from the south was higher (Fig. 8b), which may relate to low $BC/PM_{2.5}$

https://doi.org/10.5194/acp-2022-751
Preprint. Discussion started: 4 January 2023


Atmospheric Chemistry and Physics Discussions

ratios in south air masses (Xia et al., 2020). Zhang et al. (2013) found that high levels of secondary inorganic aerosols related to high humidity were transported by southern air masses, which enhanced heterogeneous reaction and leaded to relatively low BC/$PM_{2.5}$ ratios. Fig. 7b showed percentage of each cluster accounting for the total back trajectories in each year. The results indicated that variation in each cluster fraction from 2018 to 2021 was slight. In general, cluster 1-5 accounted for 19%-21%, 13%-17%, 16%-20%, 29%-36%, 12%-20% of total back trajectories, respectively. Notably, the percentage of polluted-relevant air masses (cluster 4 and cluster 5) was ~50% each year, indicating that the transport from the south and the west of has a considerable impact on the aerosol optical properties. Higher σ_{ab} and $PM_{2.5}$ mass concentrations were mainly distributed in clusters 4 and 5 in each year. σ_{ab} and $PM_{2.5}$ corresponding to clusters 4 and 5 decreased evidently from 2018 to 2021 (Fig. 8a, d), which may result from the control of source emissions in surrounding regions of Beijing. Therefore, the comprehensive control of atmospheric pollution in Beijing and surrounding regions would be highly effective in reducing air pollution in Beijing.

4 Conclusions

In this study, 4-year measurements of aerosol absorption properties and single scattering albedo for PM_{10} and PM_1 in Beijing were analyzed. The annual mean σ_{ab} of PM_{10} and PM_1 decreased by 55.0% and 53.5%, respectively, and it showed a similar decreasing trend in all seasons. SSA at 550 nm increased from 0.89 ± 0.04 for PM_{10} (0.87 ± 0.05 for PM_1) in 2018 to 0.93 ± 0.03 for PM_{10} (0.91 ± 0.04 for PM_1) in 2021 and the seasonal averages of SSA for two sizes also increased in four seasons. These results imply that absorbing aerosols are effectively controlled due to pollution control measure-taking. On

https://doi.org/10.5194/acp-2022-751
Preprint. Discussion started: 4 January 2023


Atmospheric Chemistry and Physics Discussions

the other hand, increasing SSA also implied that scattering aerosols play a more important role in radiative forcing in urban Beijing. During the study period, the annual average of Rab increased year by year and was up to 89.2% in 2021**,** indicating that fine particles are the main contributors to the total PM_{10} particle absorption, and the contributions from fine particles to absorption became more important in Beijing.

During the study period, AAE was lowest in summer and highest in winter. Seasonal mean AAE in summer was generally close to 1 indicating that freshly emitted BC from traffic sources was a major component of light-absorbing aerosols. Highest AAE highlights the importance of BrC light absorption in winter. Notably, AAE in winter decreased from 2018 to 2021, implying a decreasing contribution from BrC to absorption, which may relate to the effect control of biomass burning and coal combustion caused by changes in heating energy structure. AAE in spring and autumn was similar, indicating light-absorbing aerosols were from similar emission sources in these two seasons.

Using a simple analytical equation, we investigated the aerosol radiative effect. Aerosol radiative forcing efficiency (RFE) for PM_{10} and PM_1 was always negative, suggesting that the aerosols measured in urban Beijing have a stable cooling effect on the climate. RFE for PM_{10} and PM_1 were −27.0 and -26.2 W m^{-2} AOD^{-1} in 2021 in urban Beijing. RFE was influenced by SSA and b. Higher b corresponds to more negative RFE suggesting that smaller particles larger would cool the atmosphere more efficiently. When SSA<0.92, the absolute value of mean RFE increased by 1.59 times, suggesting that SSA plays an important role in strengthening cooling efficiency. When SSA>0.92, the mean RFE keeps relatively constant, suggesting that the intrinsic nature of the aerosol will not significantly affect the calculation of RFE. SSA increased from 0.89 to 0.93, while the

https://doi.org/10.5194/acp-2022-751
Preprint. Discussion started: 4 January 2023


Atmospheric Chemistry and Physics Discussions

yearly mean value of b was 0.13 every year during the study period. RFE became more negative from 2018 to 2021, suggesting that the efficiency of the aerosol cooling atmosphere was higher, which was mainly influenced by increasing SSA.

Regional transport and its impact on aerosol optical properties were also analyzed. The air mass back trajectories arriving at Beijing were divided into five clusters. Clusters 1, 2, and 3, which originated from the clean area in Mongolia and eastern Inner Mongolia, were transported to Beijing along the pathway with low emissions, corresponding to low σ_{ab} and low $PM_{2.5}$. Air masses from south and west (Cluster 4 and Cluster 5), which both crossed the polluted region, always brought high $PM_{2.5}$ concentrations and σ_{ab}. σ_{ab} and $PM_{2.5}$ corresponding to clusters 4 and 5 decreased evidently from 2018 to 2021, which may result from the control of source emissions in surrounding regions of Beijing. Therefore, comprehensive control of atmospheric pollution in surrounding regions of Beijing is conducive to reducing pollution in Beijing.

Data availability.

The data in this study are available at: https://doi.org/10.5281/zenodo.7466069 (Hu et al., 2022)

Competing interests.

The authors declare that they have no conflict of interest.

https://doi.org/10.5194/acp-2022-751
Preprint. Discussion started: 4 January 2023

Author contributions.

XYH analyzed the data, prepared the figures and wrote the manuscript. JYS designed the research and outlined the manuscript. XYH, CX, and JYS conducted the measurements. All co-authors discussed the results and commented on the manuscript.

Acknowledgments.

This study was supported by the National Natural Science Foundation of China (42090031, 41875147, 42075082), Chinese Academy of Meteorological Sciences (2022KJ002, 2020KJ001, 2020Z002). It was also supported by the Innovation Team for Haze-fog Observation and Forecasts of MOST.

References

Andrews, E., Ogren, J. A., Bonasoni, P., Marinoni, A., Cuevas, E., Rodríguez, S., Sun, J. Y., Jaffe, D. A., Fischer, E. V., Baltensperger, U., Weingartner, E., Coen, M. C., Sharma, S., Macdonald, A. M., Leaitch, W. R., Lin, N. H., Laj, P., Arsov, T., Kalapov, I., Jefferson, A., and Sheridan, P.: Climatology of aerosol radiative properties in the free troposphere, Atmos. Res., 102, 365-393, 10.1016/j.atmosres.2011.08.017, 2011.

Bergin, M. H., Cass, G. R., Xu, J., Fang, C., Zeng, L. M., Yu, T., Salmon, L. G., Kiang, C. S., Tang, X. Y., Zhang, Y. H., and Chameides, W. L.: Aerosol radiative, physical, and chemical properties in Beijing during June 1999, J. Geophys. Res., 106, 17969-17980, 10.1029/2001jd900073, 2001.

Bond, T. C., Anderson, T. L., and Campbell, D.: Calibration and Intercomparison of Filter-Based Measurements of Visible Light Absorption by Aerosols, Aerosol Sci. Technol., 30, 582-600, 10.1080/027868299304435, 1999.

https://doi.org/10.5194/acp-2022-751
Preprint. Discussion started: 4 January 2023

Bond, T. C., and Bergstrom, R. W.: Light Absorption by Carbonaceous Particles: An Investigative Review, Aerosol Sci. Technol., 40, 27-67, 10.1080/02786820500421521, 2007.

Bond, T. C., Doherty, S. J., Fahey, D. W., Forster, P. M., Berntsen, T., DeAngelo, B. J., Flanner, M. G., Ghan, S., Kärcher, B., Koch, D., Kinne, S., Kondo, Y., Quinn, P. K., Sarofim, M. C., Schultz, M. G., Schulz, M., Venkataraman, C., Zhang, H., Zhang, S., Bellouin, N., Guttikunda, S. K., Hopke, P. K., Jacobson, M. Z., Kaiser, J. W., Klimont, Z., Lohmann, U., Schwarz, J. P., Shindell, D., Storelvmo, T., Warren, S. G., and Zender, C. S.: Bounding the role of black carbon in the climate system: A scientific assessment, J. Geophys. Res.-Atmos., 118, 5380-5552, 10.1002/jgrd.50171, 2013.

Charlson, R. J., Schwartz, S. E., Hales, J. M., Cess, R. D., Coakley, J. A., Hansen, J. E., and Hofmann, D. J.: Climate Forcing by Anthropogenic Aerosols, Science, 255, 423-430, 10.1126/science.255.5043.423, 1992.

Collaud Coen, M., Andrews, E., Asmi, A., Baltensperger, U., Bukowiecki, N., Day, D., Fiebig, M., Fjaeraa, A. M., Flentje, H., Hyvärinen, A., Jefferson, A., Jennings, S. G., Kouvarakis, G., Lihavainen, H., Lund Myhre, C., Malm, W. C., Mihapopoulos, N., Molenar, J. V., amp, apos, Dowd, C., Ogren, J. A., Schichtel, B. A., Sheridan, P., Virkkula, A., Weingartner, E., Weller, R., and Laj, P.: Aerosol decadal trends – Part 1: In-situ optical measurements at GAW and IMPROVE stations, Atmos. Chem. Phys., 13, 869-894, 10.5194/acp-13-869-2013, 2013.

Davies, N. W., Fox, C., Szpek, K., Cotterell, M. I., Taylor, J. W., Allan, J. D., Williams, P. I., Trembath, J., Haywood, J. M., and Langridge, J. M.: Evaluating biases in filter-based aerosol absorption measurements using photoacoustic spectroscopy, Atmos. Meas. Tech.,

https://doi.org/10.5194/acp-2022-751
Preprint. Discussion started: 4 January 2023

12, 3417-3434, 10.5194/amt-12-3417-2019, 2019.

Delene, D. J., and Ogren, J. A.: Variability of Aerosol Optical Properties at Four North American Surface Monitoring Sites, J. Aerosol Sci., 59, 1135-1150, 10.1175/1520-0469(2002)059<1135:VOAOPA>2.0.CO;2, 2002.

Draxler, R. R., and Hess, G. D.: An overview of the HYSPLIT_4 modelling system of trajectories, dispersion, and deposition, Aust. Meteor. Mag., 47, 295-308, 1998.

Dubovik, O., Holben, B., Eck, T. F., Smirnov, A., Kaufman, Y. J., King, M. D., Tanre, D., and Slutsker, I.: Variability of absorption and optical properties of key aerosol types observed in worldwide locations, Journal of the Atmospheric Sciences, 59, 590-608, Doi 10.1175/1520-0469(2002)059<0590:Voaaop>2.0.Co;2, 2002.

Dumka, U. C., Kaskaoutis, D. G., Srivastava, M. K., and Devara, P. C. S.: Scattering and absorption properties of near-surface aerosol over Gangetic–Himalayan region: the role of boundary-layer dynamics and long-range transport, Atmospheric Chemistry and Physics, 15, 1555-1572, 10.5194/acp-15-1555-2015, 2015.

Ealo, M., Alastuey, A., Pérez, N., Ripoll, A., Querol, X., and Pandolfi, M.: Impact of aerosol particle sources on optical properties in urban, regional and remote areas in the north-western Mediterranean, Atmos. Chem. Phys., 18, 1149-1169, 10.5194/acp-18-1149-2018, 2018.

Garland, R. M., Schmid, O., Nowak, A., Achtert, P., Wiedensohler, A., Gunthe, S. S., Takegawa, N., Kita, K., Kondo, Y., and Hu, M.: Aerosol optical properties observed during Campaign of Air Quality Research in Beijing 2006 (CAREBeijing-2006): Characteristic differences between the inflow and outflow of Beijing city air, J. Geophys. Res., 114, D00G04, 10.1029/2008JD010780, 2009.

https://doi.org/10.5194/acp-2022-751
Preprint. Discussion started: 4 January 2023

Gui, K., Yao, W., Che, H., An, L., Zheng, Y., Li, L., Zhao, H., Zhang, L., Zhong, J., Wang, Y., and Zhang, X.: Record-breaking dust loading during two mega dust storm events over northern China in March 2021: aerosol optical and radiative properties and meteorological drivers, Atmos. Chem. Phys., 22, 7905-7932, 10.5194/acp-22-7905-2022, 2022.

Guo, J., Miao, Y., Zhang, Y., Liu, H., Li, Z., Zhang, W., He, J., Lou, M., Yan, Y., Bian, L., and Zhai, P.: The climatology of planetary boundary layer height in China derived from radiosonde and reanalysis data, Atmos. Chem. Phys., 16, 13309-13319, 10.5194/acp-16-13309-2016, 2016.

Han, T., Xu, W., Li, J., Freedman, A., Zhao, J., Wang, Q., Chen, C., Zhang, Y., Wang, Z., Fu, P., Liu, X., and Sun, Y.: Aerosol optical properties measurements by a CAPS single scattering albedo monitor: Comparisons between summer and winter in Beijing, China, J. Geophys. Res.-Atmos., 122, 2513-2526, 10.1002/2016jd025762, 2017.

Haywood, J. M., and Shine, K. P.: The effect of anthropogenic sulfate and soot aerosol on the clear sky planetary radiation budget, Geophys. Res. Lett., 22(5), 603-606, 10.1029/95GL00075, 1995.

He, X., Li, C. C., Lau, A. K. H., Deng, Z. Z., Mao, J. T., Wang, M., and Liu, X., Y.: An intensive study of aerosol optical properties in Beijing urban area, Atmos. Chem. Phys., 9, 8903-8915, 10.5194/acp-9-8903-2009, 2009.

Helin, A., Virkkula, A., Backman, J., Pirjola, L., Sippula, O., Aakko-Saksa, P., Väätäinen, S., Mylläri, F., Järvinen, A., Bloss, M., Aurela, M., Jakobi, G., Karjalainen, P., Zimmermann, R., Jokiniemi, J., Saarikoski, S., Tissari, J., Rönkkö, T., Niemi, J. V., and Timonen, H.: Variation of Absorption Ångström Exponent in Aerosols From Different Emission Sources, J. Geophys. Res.-Atmos., 126, 10.1029/2020jd034094, 2021.

https://doi.org/10.5194/acp-2022-751
Preprint. Discussion started: 4 January 2023


Atmospheric Chemistry and Physics Discussions

Hu, X., Sun, J., Xia, C., Shen, X., Zhang, Y., Zhang, X., and Zhang, S.: Simultaneous measurements of PM1 and PM10 aerosol scattering properties and their relationships in urban Beijing: A two-year observation, Sci. Total Environ., 770, 145215, 10.1016/j.scitotenv.2021.145215, 2021.

Hu, X., Sun, J., Xia, C., Shen, X., Zhang, Y., Liu, Q., Liu, Z., Zhang, S., Wang, J., Yu, A., Lu, J., Liu, S., and Zhang, X.: Rapid decline of aerosol absorption coefficient and aerosol optical properties effects on radiative forcing in urban areas of Beijing from 2018 to 2021 [Data set], Zenodo, https://doi.org/10.5281/zenodo.7466069, 2022.

J. Hansen, M. Sato, and Ruedy, R.: Radiative forcing and climate response, J. Geophys. Res., 102, 6831-6864, 10.1029/96jd03436, 1997.

Jacobson, M. Z.: Strong radiative heating due to the mixing state of black carbon in atmospheric aerosols, Nature, 409, 695-697, 10.1038/35055518, 2001.

Ji, D., Gao, W., Maenhaut, W., He, J., Wang, Z., Li, J., Du, W., Wang, L., Sun, Y., Xin, J., Hu, B., and Wang, Y.: Impact of air pollution control measures and regional transport on carbonaceous aerosols in fine particulate matter in urban Beijing, China: insights gained from long-term measurement, Atmos. Chem. Phys., 19, 8569-8590, 10.5194/acp-19-8569-2019, 2019.

Ji, D., Li, J., Shen, G., He, J., Gao, W., Tao, J., Liu, Y., Tang, G., Zeng, L., Zhang, R., and Wang, Y.: Environmental effects of China's coal ban policy: Results from in situ observations and model analysis in a typical rural area of the Beijing-Tianjin-Hebei region, China, Atmos. Res., 268, 10.1016/j.atmosres.2022.106015, 2022.

Jing, J., Wu, Y., Tao, J., Che, H., Xia, X., Zhang, X., Yan, P., Zhao, D., and Zhang, L.: Observation and analysis of near-surface atmospheric aerosol optical properties in urban

https://doi.org/10.5194/acp-2022-751
Preprint. Discussion started: 4 January 2023

Beijing, Particuology, 18, 144-154, 10.1016/j.partic.2014.03.013, 2015.

Lack, D. A., and Cappa, C. D.: Impact of brown and clear carbon on light absorption enhancement, single scatter albedo and absorption wavelength dependence of black carbon, Atmos. Chem. Phys., 10, 4207-4220, 10.5194/acp-10-4207-2010, 2010.

Lee, K. H., Li, Z., Wong, M. S., Xin, J., Wang, Y., Hao, W.-M., and Zhao, F.: Aerosol single scattering albedo estimated across China from a combination of ground and satellite measurements, J. Geophys. Res., 112, 10.1029/2007jd009077, 2007.

Lei, L., Zhou, W., Chen, C., He, Y., Li, Z., Sun, J., Tang, X., Fu, P., Wang, Z., and Sun, Y.: Long-term characterization of aerosol chemistry in cold season from 2013 to 2020 in Beijing, China, Environ. Pollut., 268, 115952, 10.1016/j.envpol.2020.115952, 2021.

Li, J., Carlson, B. E., Yung, Y. L., Lv, D., Hansen, J., Penner, J. E., Liao, H., Ramaswamy, V., Kahn, R. A., Zhang, P., Dubovik, O., Ding, A., Lacis, A. A., Zhang, L., and Dong, Y.: Scattering and absorbing aerosols in the climate system, Nature Reviews Earth & Environment, 10.1038/s43017-022-00296-7, 2022a.

Li, W., Liu, X., Duan, F., Qu, Y., and An, J.: A one-year study on black carbon in urban Beijing: Concentrations, sources and implications on visibility, Atmos. Pollut. Res., 13, 10.1016/j.apr.2021.101307, 2022b.

Liu, G. J., Xin, J. Y., Wang, X., Si, R. R., Ma, Y. N., Wen, T. X., Zhao, L., Zhao, D. D., Wang, Y. S., and Gao, W. K.: Impact of the coal banning zone on visibility in the Beijing-Tianjin-Hebei region, Sci. Total Environ., 692, 402-410, 10.1016/j.scitotenv.2019.07.006, 2019.

Luo, L., Tian, H., Liu, H., Bai, X., Liu, W., Liu, S., Wu, B., Lin, S., Zhao, S., Hao, Y., Sun, Y., Hao, J., and Zhang, K.: Seasonal variations in the mass characteristics and optical

https://doi.org/10.5194/acp-2022-751
Preprint. Discussion started: 4 January 2023

properties of carbonaceous constituents of PM2.5 in six cities of North China, Environ. Pollut., 268, 115780, 10.1016/j.envpol.2020.115780, 2020.

Luoma, K., Virkkula, A., Aalto, P., Petäjä, T., and Kulmala, M.: Over a 10-year record of aerosol optical properties at SMEAR II, Atmos. Chem. Phys., 19, 11363-11382, 10.5194/acp-19-11363-2019, 2019.

Moosmüller, H., Chakrabarty, R. K., and Arnott, W. P.: Aerosol light absorption and its measurement: A review, J. Quant. Spectrosc. Radiat. Transf., 110, 844-878, 10.1016/j.jqsrt.2009.02.035, 2009.

Ogren, J. A., Wendell, J., Andrews, E., and Sheridan, P. J.: Continuous light absorption photometer for long-term studies, Atmos. Meas. Tech., 10, 4805-4818, 10.5194/amt-10-4805-2017, 2017.

Ran, L., Deng, Z. Z., Wang, P. C., and Xia, X. A.: Black carbon and wavelength-dependent aerosol absorption in the North China Plain based on two-year aethalometer measurements, Atmos. Environ., 142, 132-144, 10.1016/j.atmosenv.2016.07.014, 2016.

Segura, S., Estellés, V., Esteve, A. R., Marcos, C. R., Utrillas, M. P., and Martínez-Lozano, J. A.: Multiyear in-situ measurements of atmospheric aerosol absorption properties at an urban coastal site in western Mediterranean, Atmos. Environ., 129, 18-26, 10.1016/j.atmosenv.2016.01.008, 2016.

Shen, Y., Virkkula, A., Ding, A., Wang, J., Chi, X., Nie, W., Qi, X., Huang, X., Liu, Q., Zheng, L., Xu, Z., Petäjä, T., Aalto, P. P., Fu, C., and Kulmala, M.: Aerosol optical properties at SORPES in Nanjing, east China, Atmos. Chem. Phys., 18, 5265-5292, 10.5194/acp-18-5265-2018, 2018.

Sheridan, P. J., and Ogren, J. A.: Observations of the vertical and regional variability of

https://doi.org/10.5194/acp-2022-751
Preprint. Discussion started: 4 January 2023

aerosol optical properties over central and eastern North America, J. Geophys. Res., 104, 16793-16805, 10.1029/1999jd900241, 1999.

Sun, J., Wang, Z., Zhou, W., Xie, C., Wu, C., Chen, C., Han, T., Wang, Q., Li, Z., Li, J., Fu, P., Wang, Z., and Sun, Y.: Measurement report: Long-term changes in black carbon and aerosol optical properties from 2012 to 2020 in Beijing, China, Atmos. Chem. Phys., 22, 561-575, 10.5194/acp-22-561-2022, 2022.

Sun, Y., Xu, W., Zhang, Q., Jiang, Q., Canonaco, F., Prévôt, A. S. H., Fu, P., Li, J., Jayne, J., Worsnop, D. R., and Wang, Z.: Source apportionment of organic aerosol from 2-year highly time-resolved measurements by an aerosol chemical speciation monitor in Beijing, China, Atmos. Chem. Phys., 18, 8469-8489, 10.5194/acp-18-8469-2018, 2018.

Sun, Y., Lei, L., Zhou, W., Chen, C., He, Y., Sun, J., Li, Z., Xu, W., Wang, Q., Ji, D., Fu, P., Wang, Z., and Worsnop, D. R.: A chemical cocktail during the COVID-19 outbreak in Beijing, China: Insights from six-year aerosol particle composition measurements during the Chinese New Year holiday, Sci Total Environ, 742, 140739, 10.1016/j.scitotenv.2020.140739, 2020.

Szopa, S., Naik, V., Adhikary, B., Artaxo, P., Berntsen, T., Collins, W. D., Fuzzi, S., Gallardo, L., Kiendler-Scharr, A., Klimont, Z., Liao, H., Unger, N., and Zanis, P.: Short-Lived Climate Forcers. In Climate Change 2021: The Physical Science Basis. Contribution of Working Group I to the Sixth Assessment Report of the Intergovernmental Panel on Climate Change [Masson-Delmotte, V., P. Zhai, A. Pirani, S.L. Connors, C. Péan, S. Berger, N. Caud, Y. Chen, L. Goldfarb, M.I. Gomis, M. Huang, K. Leitzell, E. Lonnoy, J.B.R. Matthews, T.K. Maycock, T. Waterfield, O. Yelekçi, R. Yu, and B. Zhou (eds.)], Cambridge University Press, Cambridge, United Kingdom and New York, NY, USA, 817-922,

https://doi.org/10.5194/acp-2022-751
Preprint. Discussion started: 4 January 2023

585 10.1017/9781009157896.008, 2021.

Tuch, T. M., Haudek, A., Müller, T., Nowak, A., Wex, H., and Wiedensohler, A.: Design and performance of an automatic regenerating adsorption aerosol dryer for continuous operation at monitoring sites, Atmos. Meas. Tech., 2, 417-422, 10.5194/amt-2-417-2009, 2009.

590 Twomey, S.: Pollution and the Planetary Albedo, Atmos. Environ., 41, 120-125, 10.1016/j.atmosenv.2007.10.062, 2007.

Virkkula, A., Backman, J., Aalto, P. P., Hulkkonen, M., Riuttanen, L., Nieminen, T., dal Maso, M., Sogacheva, L., de Leeuw, G., and Kulmala, M.: Seasonal cycle, size dependencies, and source analyses of aerosol optical properties at the SMEAR II

595 measurement station in Hyytiälä, Finland, Atmos. Chem. Phys., 11, 4445-4468, 10.5194/acp-11-4445-2011, 2011.

Vu, T. V., Shi, Z., Cheng, J., Zhang, Q., He, K., Wang, S., and Harrison, R. M.: Assessing the impact of clean air action on air quality trends in Beijing using a machine learning technique, Atmospheric Chemistry and Physics, 19, 11303-11314, 10.5194/acp-19-11303-

600 2019, 2019.

Wang, Q. L., Wang, L. L., Gong, C. S., Li, M. G., Xin, J. Y., Tang, G. Q., Sun, Y., Gao, J. H., Wang, Y. H., Wu, S., Kang, Y. Y., Yang, Y., Li, T. T., Liu, J. D., and Wang, Y. S.: Vertical evolution of black and brown carbon during pollution events over North China Plain, Sci. Total Environ., 806, ARTN 150950

605 10.1016/j.scitotenv.2021.150950, 2022.

Wang, T., Du, Z., Tan, T., Xu, N., Hu, M., Hu, J., and Guo, S.: Measurement of aerosol optical properties and their potential source origin in urban Beijing from 2013-2017, Atmos.

https://doi.org/10.5194/acp-2022-751
Preprint. Discussion started: 4 January 2023

Environ., 206, 293-302, 10.1016/j.atmosenv.2019.02.049, 2019.

Wang, Y. Q., Zhang, X. Y., and Draxler, R. R.: TrajStat: GIS-based software that uses various trajectory statistical analysis methods to identify potential sources from long-term air pollution measurement data, Environ. Model Softw., 24, 938-939, 10.1016/j.envsoft.2009.01.004, 2009.

WMO/GAW: WMO/GAW Aerosol Measurement Procedures, Guidelines and Recommendations, Geneva, Switzerland, 2016.

Xia, C., Sun, J., Qi, X., Shen, X., Zhong, J., Zhang, X., Wang, Y., Zhang, Y., and Hu, X.: Observational study of aerosol hygroscopic growth on scattering coefficient in Beijing: A case study in March of 2018, Sci. Total Environ., 685, 239-247, 10.1016/j.scitotenv.2019.05.283, 2019.

Xia, Y., Wu, Y., Huang, R. J., Xia, X., Tang, J., Wang, M., Li, J., Wang, C., Zhou, C., and Zhang, R.: Variation in black carbon concentration and aerosol optical properties in Beijing: Role of emission control and meteorological transport variability, Chemosphere, 254, 126849, 10.1016/j.chemosphere.2020.126849, 2020.

Xie, C., He, Y., Lei, L., Zhou, W., Liu, J., Wang, Q., Xu, W., Qiu, Y., Zhao, J., Sun, J., Li, L., Li, M., Zhou, Z., Fu, P., Wang, Z., and Sun, Y.: Contrasting mixing state of black carbon-containing particles in summer and winter in Beijing, Environ. Pollut., 263, 114455, 10.1016/j.envpol.2020.114455, 2020.

Xu, X., and Zhang, T.: Spatial-temporal variability of PM2.5 air quality in Beijing, China during 2013-2018, J. Environ. Manag., 262, 110263, 10.1016/j.jenvman.2020.110263, 2020.

Yi, Z., Wang, Y., Chen, W., Guo, B., Zhang, B., Che, H., and Zhang, X.: Classification of

https://doi.org/10.5194/acp-2022-751
Preprint. Discussion started: 4 January 2023

the Circulation Patterns Related to Strong Dust Weather in China Using a Combination of the Lamb–Jenkinson and k-Means Clustering Methods, Atmosphere, 12, 10.3390/atmos12121545, 2021.

Zhang, Q., Zheng, Y., Tong, D., Shao, M., Wang, S., Zhang, Y., Xu, X., Wang, J., He, H., Liu, W., Ding, Y., Lei, Y., Li, J., Wang, Z., Zhang, X., Wang, Y., Cheng, J., Liu, Y., Shi, Q., Yan, L., Geng, G., Hong, C., Li, M., Liu, F., Zheng, B., Cao, J., Ding, A., Gao, J., Fu, Q., Huo, J., Liu, B., Liu, Z., Yang, F., He, K., and Hao, J.: Drivers of improved $PM_{2.5}$ air quality in China from 2013 to 2017, P. Natl. Acad. Sci. USA, 116, 24463-24469, 10.1073/pnas.1907956116, 2019.

Zhang, R., Jing, J., Tao, J., Hsu, S. C., Wang, G., Cao, J., Lee, C. S. L., Zhu, L., Chen, Z., Zhao, Y., and Shen, Z.: Chemical characterization and source apportionment of PM2.5 in Beijing: seasonal perspective, Atmos. Chem. Phys., 13, 7053-7074, 10.5194/acp-13-7053-2013, 2013.

Zhang, Y. Z., Zhi, G. R., Jin, W. J., Wang, L., Guo, S. C., Shi, R., Sun, J. Z., Cheng, M. M., Bi, F., Gao, J., Zhang, B. J., Wu, J. J., Shi, Z. H., Liu, B., Wang, Z., and Li, S. Y.: Differing effects of escalating pollution on absorption and scattering efficiencies of aerosols: Toward co-beneficial air quality enhancement and climate protection measures, Atmos. Environ., 232, 10.1016/j.atmosenv.2020.117570, 2020.

Zhao, S. M., Hu, B., Du, C. J., Tang, L. Q., Ma, Y. J., Liu, H., Zou, J. N., Liu, Z. R., Wei, J., and Wang, Y. S.: Aerosol optical characteristics and radiative forcing in urban Beijing, Atmos. Environ., 212, 41-53, 10.1016/j.atmosenv.2019.05.034, 2019.

Zhao, S. M., Hu, B., Gao, W. K., Li, L. C., Huang, W., Wang, L. L., Yang, Y., Liu, J. D., Li, J. Y., Ji, D. S., Zhang, R. J., Zhang, Y. Y., and Wang, Y. S.: Effect of the "coal to gas" project

https://doi.org/10.5194/acp-2022-751
Preprint. Discussion started: 4 January 2023

Atmospheric Chemistry and Physics Discussions

on atmospheric NOX during the heating period at a suburban site between Beijing and Tianjin, Atmos. Res., 241, 10.1016/j.atmosres.2020.104977, 2020.

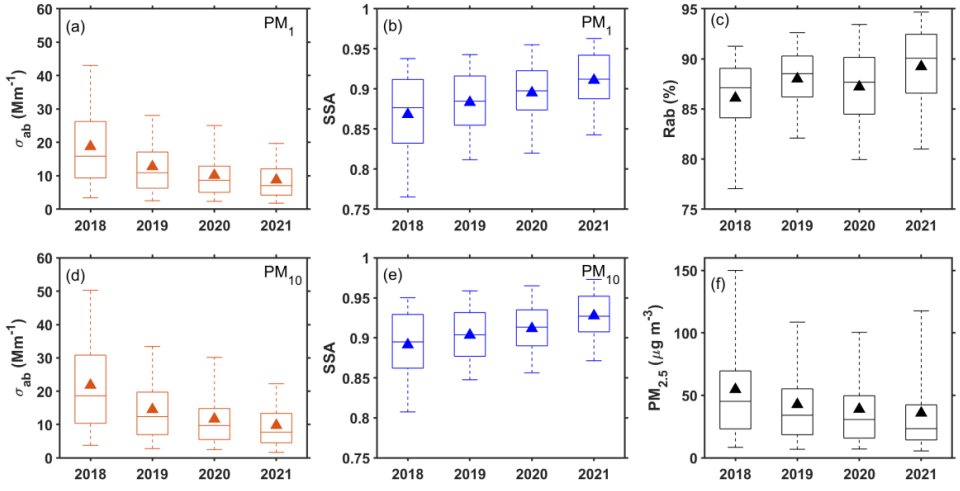

Figure 1. Annual variation of aerosol optical properties and $PM_{2.5}$ mass concentration, absorption coefficient σ_{ab} at 550 nm for (a) PM_1 and (d) PM_{10}, SSA at 550 nm for (b) PM_1 and (e) PM_{10}, (c) Rab and (f)$PM_{2.5}$ mass concentration. The solid line inside the box represents the median and the triangle indicates the mean. The box contains the range of values from 25% (bottom) to 75% (top), and the upper and lower whiskers are the 95th and 5th percentiles, respectively.

https://doi.org/10.5194/acp-2022-751
Preprint. Discussion started: 4 January 2023

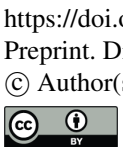

Atmospheric Chemistry and Physics Discussions

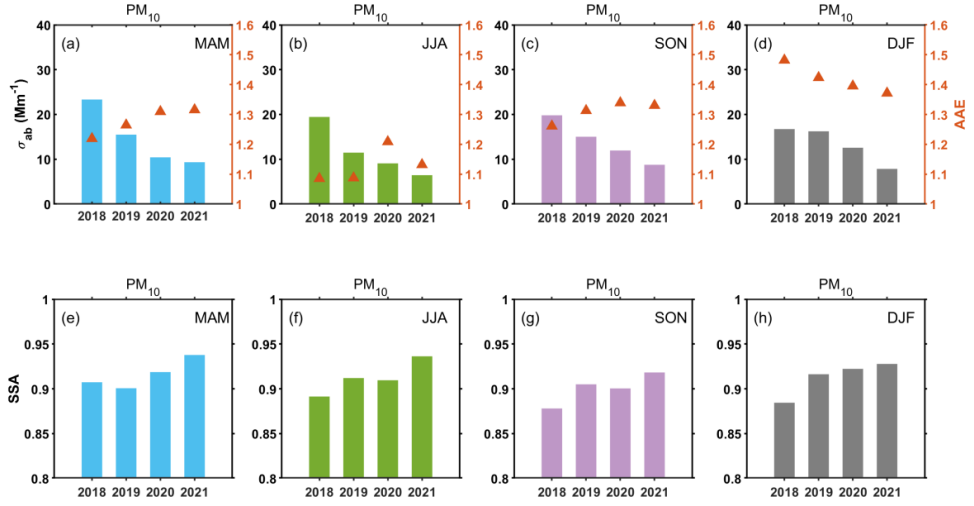

Figure 2. Seasonal variation of aerosol optical properties of PM_{10} from 2018-2021, (a-d) σ_{ab} (bar) at 550 nm, $AAE_{450/700}$ (triangle), and (e-h) SSA (bar) at 550 nm.

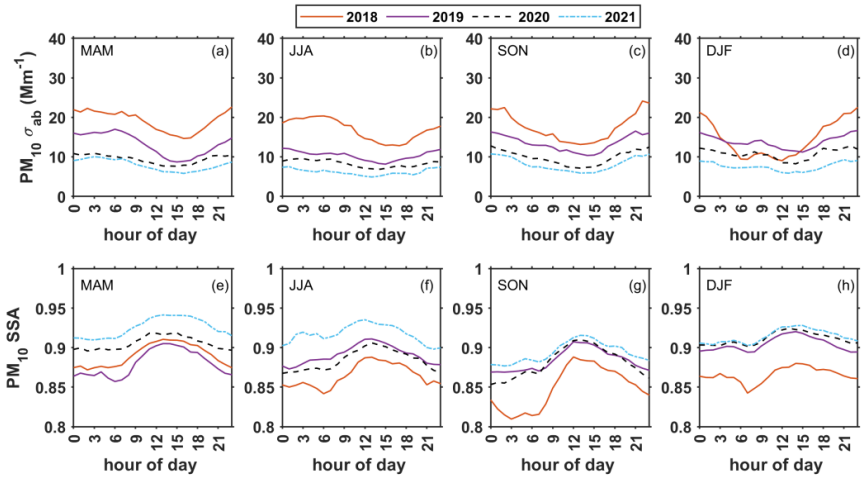

Figure 3. Diurnal variations of σ_{ab} (a-d) and SSA (e-h) at 550 nm for PM_{10} in four seasons from 2018 to 2021.

https://doi.org/10.5194/acp-2022-751
Preprint. Discussion started: 4 January 2023

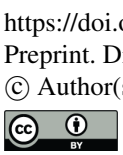

Atmospheric Chemistry and Physics Discussions

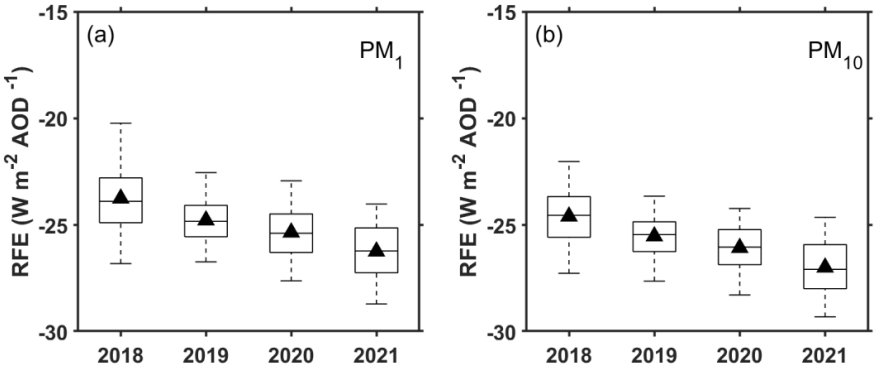

Figure 4. The annual variation of aerosol radiative forcing efficiency for PM_1 (a) and PM_{10} (b). The solid line inside the box represents the median, and the triangle indicates the mean. The box contains the range of values from 25% (bottom) to 75% (top), and the 95th and 5th percentiles, respectively.

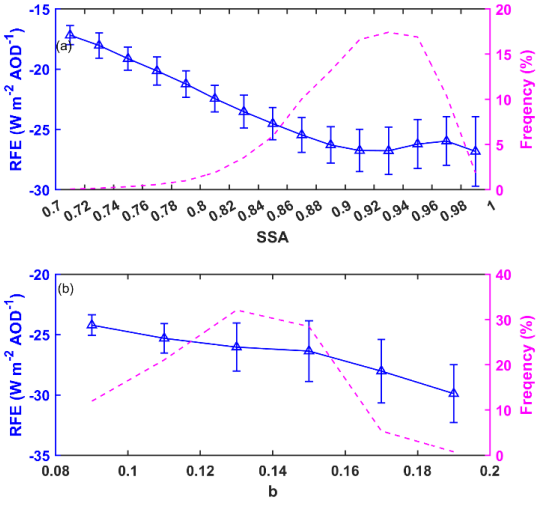

Figure 5. The relationship of RFE with (a) SSA and (b) backscattering ratio. The pink dash line represents the frequency distribution of SSA (a) and backscattering ratio (b).

https://doi.org/10.5194/acp-2022-751
Preprint. Discussion started: 4 January 2023

Atmospheric Chemistry and Physics Discussions

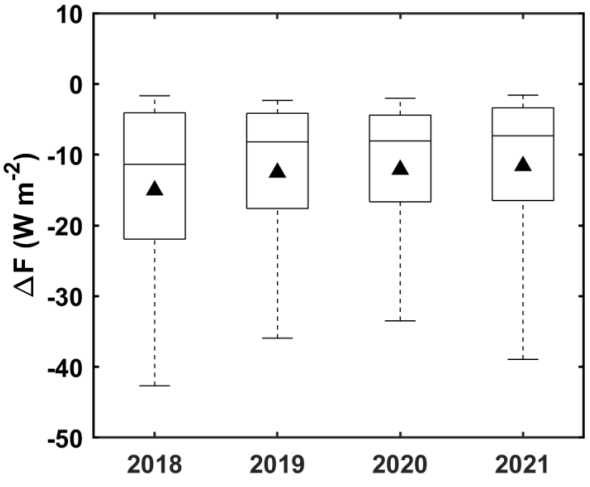

Figure 6. Annual variation of aerosol radiative forcing (ΔF) at TOA from 2018 to 2021 calculated from daily mean data. The solid line inside the box represents the median, and the triangle indicates the mean. The box contains the range of values from 25% (bottom) to 75% (top), and the 95th and 5th percentiles, respectively.

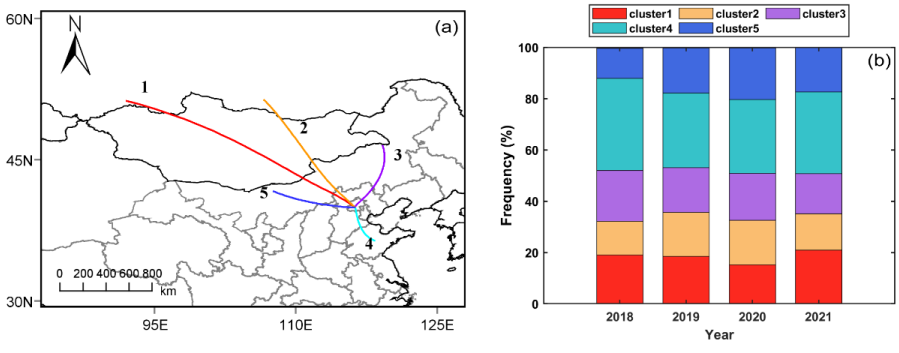

Figure 7. (a) Air mass clusters of back trajectories arriving in Beijing during 2018–2021 and (b) the fraction of each cluster accounting for the total back trajectories in each year.

https://doi.org/10.5194/acp-2022-751
Preprint. Discussion started: 4 January 2023

Atmospheric Chemistry and Physics Discussions

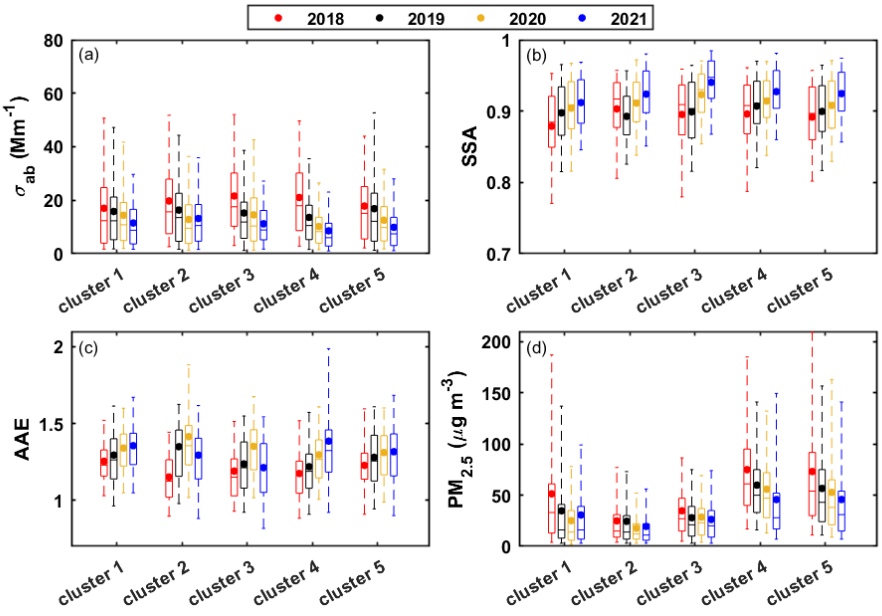

Figure 8. The variation of (a) σ_{ab}, (b) SSA, (c) AAE, and $PM_{2.5}$ mass concentration in each cluster from 2018 to 2021. The solid line inside the box represents the median and the dot indicates the mean. The box contains the range of values from 25% (bottom) to 75% (top), and the 95th and 5th percentiles, respectively.